

Green Synthesis of Piezoelectric Thin Films based on Niobium Doped Barium Zirconate Titanate – Barium Calcium Titanate (Nb-BZT-BCT)

Paola S. Barbato^{*a}, Luigi Barretta^a, Rossana Scaldaferrri^a, Paolo Aprea^b, Annachiara Esposito^a, Valeria Casuscelli^a, Domenico Caputo^b

^a Analog, MEMS & Sensors Group STMicroelectronics, Via Remo De Feo, 1 80022 Arzano, Italy

^b ACLabs - Laboratori di Chimica Applicata, DICMaPI, Università degli Studi di Napoli Federico II, P.Le V. Tecchio 80, 80125 Napoli

paolasabrina.barbato@unina.it

This work focuses on the sol-gel production of thin films made of Barium Zirconate Titanate -Barium Calcium Titanate with 2% niobium doping starting from non-toxic, non-hazardous precursor solutions. Multi-layered samples were produced by repeated chemical solution deposition routes carried out by spinning the opportune precursor solutions and then performing three heat treatments at increasing temperatures. Undoped samples have also been produced for comparison. A simplification of the process, obtained by eliminating the lowest temperature heat treatment, intended for drying the xerogel, has also been tested. The characterizations indicated that the niobium-doped sample produced with the simplified process showed a better morphology and therefore better results in terms of electrical properties.

1. Introduction

With the term of PiezoMEMS is defined a class of MEMS (Micro Electro-Mechanical Systems) in which the piezoelectric elements are mainly integrated in the form of thin films (Trolier-Mckinstry et al., 2004) with a micrometric thickness to get a series of advantages, such as reduced weight and inertia (Hu, 2018).

To date, perovskitic lead zirconate titanate (PZT), given its piezoelectric performance and operating temperature far higher than other piezoceramics, is the most widely used material, despite its PbO content being about 70% by weight and despite that, during the production, use and disposal of PZT, a series of toxic substances are released (Shen, 2018), harmful to the environment and human health. Directive 2011/65 / EU imposed limits on the lead content in consumer goods and included PZT among the hazardous materials to be replaced by safer materials. Therefore, it allows its use in strategic areas until materials with comparable performance are available. As a response to the legislative activity of the EU, the scientific community is moving towards the search for lead-free piezoelectric materials. Among the possible piezoelectric - ferroelectric candidates, the ceramic barium zirconate - titanate - barium - calcium titanate (BZT - BCT) (Aprea et al., 2017) shows a response comparable to that of PZT (Rodel et al., 2015), albeit in a narrower temperature range, representing a possible substitute for ambient temperature applications, such as energy harvesting (Khang et al., 2012).

To produce piezoelectric thin films the chemical solution deposition technique is of a great importance, and therefore is widely used, thanks to the possibility to finely tune the stoichiometry, which is particularly important for such kind of perovskitic materials having a quite complex formula (AA'BB'O₃). In order to improve the ferroelectric/piezoelectric properties (i.e. softening the behavior) a well-known strategy is donor doping, i.e. introducing cations with higher valence, such as Nb⁵⁺ that substitutes Ti⁴⁺ and Zr⁴⁺ in the B sites of the perovskitic structure, for example in the case of PZT (Akkopru-Akgun et al., 2019). Donor doping with niobium could be an effective way to improve the electrical properties of BZT-BCT piezoceramic to be compliant with the more and more stringent technical requirements of Piezo MEMS device market (Zhang et al., 2013). In this

work, we present a green deposition process to obtain niobium doped BZT-BCT thin films. Moreover, we address the impact of doping on the morphology and on some electrical properties of the thin films.

2. Materials and Methods

2.1 Precursor solution synthesis and characterizations

The precursor solution 0.35 M has been prepared starting from the reagent grade chemicals all purchased by Merck. As source of Site A metals: barium acetate ($\text{Ba}(\text{CH}_3\text{COO})_2$), calcium acetate monohydrate ($\text{Ca}(\text{CH}_3\text{COO})_2 \cdot \text{H}_2\text{O}$) were used while as source of metals of Site B: niobium ethoxide ($\text{Nb}(\text{OC}_2\text{H}_5)_5$), zirconium butoxide ($\text{Zr}(\text{OC}_4\text{H}_9)_4$) 80% solution in 1-butanol and titanium isopropoxide ($\text{Ti}(\text{OC}_3\text{H}_7)_4$) were used in stoichiometric amounts to obtain the $0.5[\text{Ba}(\text{Zr}_{0.2}\text{Ti}_{0.8})_{0.98}\text{Nb}_{0.02}\text{O}_3] - 0.5(\text{Ba}_{0.7}\text{Ca}_{0.3}\text{Ti}_{0.98}\text{Nb}_{0.02}\text{O}_3)$ solid solution. Moreover, ethylene glycol, acetic acid and 1-butanol were used as film thickener, chelating-agent, and solvent, respectively. The procedure to obtain the solution of precursor is already reported in (Casuscelli et al, 2022). Hereafter, the terms EG and EG-2% Nb will be used to denote the BZT-BCT and the Nb-doped BZT-BCT solution of precursors, respectively.

About 15 ml of both the precursor solutions were dried at 120°C , which resulted in precipitate gel formation, and subsequently analyzed by X-ray diffraction (PANalytical, X'Pert Pro).

Afterwards, the obtained powders were calcined at 1200°C to induce the formation of BZT-BCT.

White precursor powders derived from the gel were thermally analyzed by High temperature Differential Thermal/Thermogravimetric Analysis (NETZSCH, STA 409 Luxx). The temperature was scanned from room temperature to 1200°C at a heating rate of $10^\circ\text{C}/\text{min}$ under nitrogen flow.

2.2 Thin films deposition and characterization

Niobium doped BZT-BCT and undoped BZT-BCT thin films were grown by means of repeated chemical solution routes. The solution of precursors was dispensed over $400\ \mu\text{m}$ -thick Pt/TiO₂/SiO₂/Si substrate by spinning it in a spin coater (Specialty Coating Systems, model P.6712). After deposition, the drying at 150°C and pyrolysis @ 350°C steps were carried out in a slowly depressurized glove box. To obtain the desired perovskite phase, the films were calcined in a muffle at 750°C with a thermal increase of $10^\circ\text{C}/\text{min}$. After the crystallization of the first layer the deposition/ thermal treatments were repeated, and the crystallization was performed every other two layer for a total of 5 depositions. In this work we check the possibility of a process simplification by removing the drying step at 150°C , since the most part of the solvent is removed during the spin off phase (200 s @ 2000 RPM) of the spin coating process. Hence a total of 4 different thin films have been fabricated whose peculiarities are reported in Table 1.

Table 1: Properties, nomenclature, and results of the fabricated thin films

Device	Nb %	Thermal treatments	Nomenclature	Thickness nm	$\Delta P_r/\Delta E_c$ $\mu\text{C}(\text{kVcm})^{-1}$
1	0	Drying & Pyrolysis	EG; 150 – 350 – 750°C	210 – 220	0.0266
2	0	pyrolysis	EG; 350 – 750°C	210 – 220	0.0280
3	2	Drying & Pyrolysis	EG – 2% Nb; 150 – 350 – 750°C	220 – 260	0.0245
4	2	pyrolysis	EG – 2% Nb; 350 – 750°C	250 – 320	0.0310

Grazing incident x-ray diffraction ($\omega = 1^\circ$) over a 2θ range from 10 to 60° were used to assess the crystal structure of the fabricated thin films, with the following operating conditions: CuK α radiation, 40 kV, 40 mA, step size 0.0131° 2θ , counting time 18.87 s per step. While a field emission gun scanning electron microscope (FEG-SEM, SUPRA 40 Carl Zeiss) performed at an accelerating voltage of 10 kV with a 5 mm WD was used to evaluate the surface roughness and texture uniformity of the thin films at micro- and nano- scale. Final stacks made of Si/SiO₂/TiO₂/Pt(100nm)/ doped or undoped BZT_BCT thin film/Pt(100nm) were obtain by sputtering the platinum top electrode through a shadow mask obtaining square capacitors with area ranging from 0.25 to $1\ \text{mm}^2$. The contact with Pt bottom electrode was provided by manually etching the film layer with HCl 1M at 100°C . After the etching procedure, the film thickness is measured by using a profilometer (AMBIOS Technology XP-1). The Polarization (P) versus Electric field (E) loops of devices were measured at room temperature by Aixact TFAnalyzer 2000E by triangular bipolar signal at 1 kHz frequency.

3. Results

3.1 Solution of precursor characterization results

The two synthesized solutions are visually homogeneous, clear, and transparent. Furthermore, the solutions proved to be stable in a time interval of 8 months, with no precipitation or gelling.

Figure 1, report the X-ray diffraction pattern of EG and EG-2% Nb precursor dried powders. Once the solvent is evaporated, some crystalline phases mainly acetates are formed in the dried powders as visible from the numerous peaks that are present in their patterns. Even if the two pattern are similar, it appears that the Nb precursor suppresses the formation of the crystalline phase related to the peak at 7.6°, suggesting an amorphizing effect of the niobium.

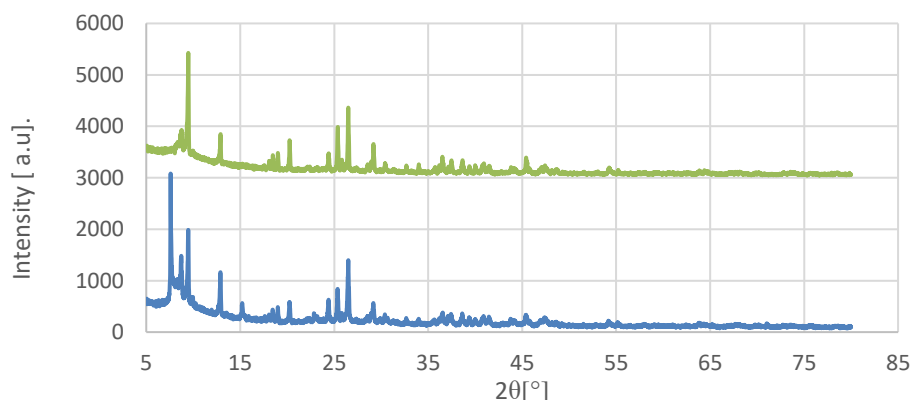


Figure 1 XRD on dried powders deriving from EG-2%Nb (green line) EG (blue line) solution.

The TG analysis is reported in Figure 2. It appears that the two solutions of precursor behave very differently.

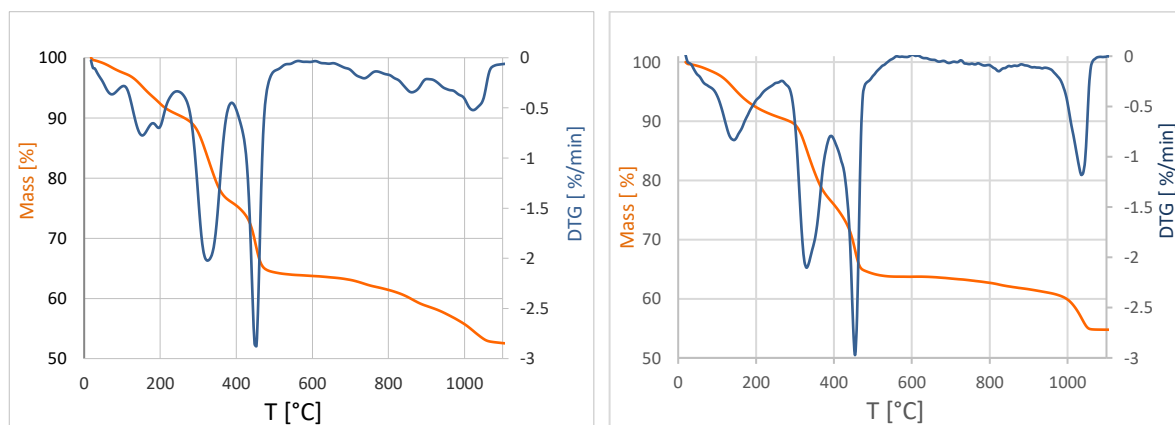
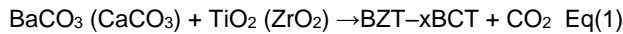


Figure 2 TGA and DTG on dried powders: a) EG-2% Nb; b) EG.

According to the work of Wang (2013) and Aprea (2017): the multiple peaks (i.e. in the range of temperature <250°C) can be attributed to the evaporation of residual solvent or alcohols produced by condensation of alkoxides reactions during gel formation. While the peaks that are in the range which extends up to 600°C are attributable to the decomposition of xerogel with the loss of organic matter, the formation of titanium (TiO_2) and zirconium oxides (ZrO_2) and, where present, niobium oxide (Nb_2O_5) and the decarboxylation of acetates to produce BaCO_3 and CaCO_3 . The last peaks at temperatures higher than 600 °C are attributable to the decomposition of carbonates which is crucial for the formation of BZT-BCT perovskite desired phase according to the solid reaction expressed in the eq.(1) and proposed by (Wang et al, 2013) for BZT-xBCT undoped perovskite:



In the case of the EG – 2%Nb solution, in line with the «amorphising» effect of niobium, the decomposition of the carbonates starts about 650 °C with a series of less defined peaks which extend up to 1000°C. For the EG solution, on the other hand, the decomposition of the carbonates does not take place before approximately 900 °C, thus hindering the formation of the desired perovskitic phase.

3.2 Thin films' crystal structure and morphology results.

In Figure 3 are reported the XRD patterns of the BZT -BCT doped (Figure 3 c) and d)) and undoped thin films (Figure 3 a) and b)) with the different thermal treatments (Figure 3 b) and d) pyrolysis; a) and c) drying and pyrolysis). The obtained patterns are compatible with the presence of pure non-oriented perovskitic phase according to the previous work (Barbato et al. 2021, a & b) and the literature (Wang et al. 2013, Kang et al. 2012). In the case of the niobium-containing samples it appears that the peaks are slightly narrower, which could indicate a larger mean crystalline domain size than in the niobium-free samples, although given the noisiness of the signal and the possible surface roughness of the thin films, it cannot be determined with certainty. This effect could be related to the amorphising effect of niobium and the relative TGA analysis showing a more facile decomposition of carbonates in the niobium containing sample, moreover niobium can act as sintering aid as stated by Zhang and coworkers (2013). In fact, Nb⁵⁺ is incorporated into the perovskite lattice eventually substituting Ti⁴⁺ due to the similar ionic radius (0,064nm vs 0,068nm respectively). Comparing films made of the same material but with different thermal treatments, no clear evidence of the improvements of the crystallinity degree by drying have been obtained supporting the hypothesis that the great part of the solvents is evaporated during the spin coating step.

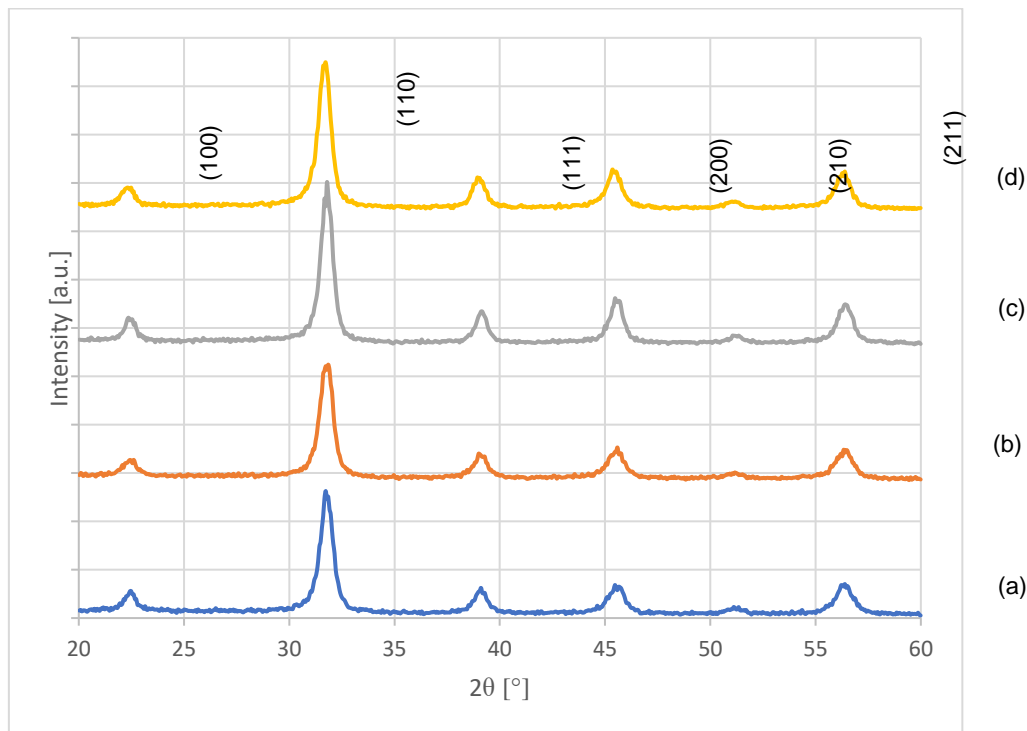


Figure 3 XRD patterns in grazing angles ($\omega=1$): a) EG; 150 – 350 – 750°C; b) EG; 350 – 750°C; c) EG – 2% Nb; 150 – 350 – 750°C; d) EG – 2% Nb; 350 – 750°C.

BZT-BCT doped and undoped thin films are characterized by numerous defectivities coming from the manual and non-standardized process (not shown). Nevertheless, nanograins are quite homogeneous as evidenced in the Figure 4 for which some pores and cracks are also visible.

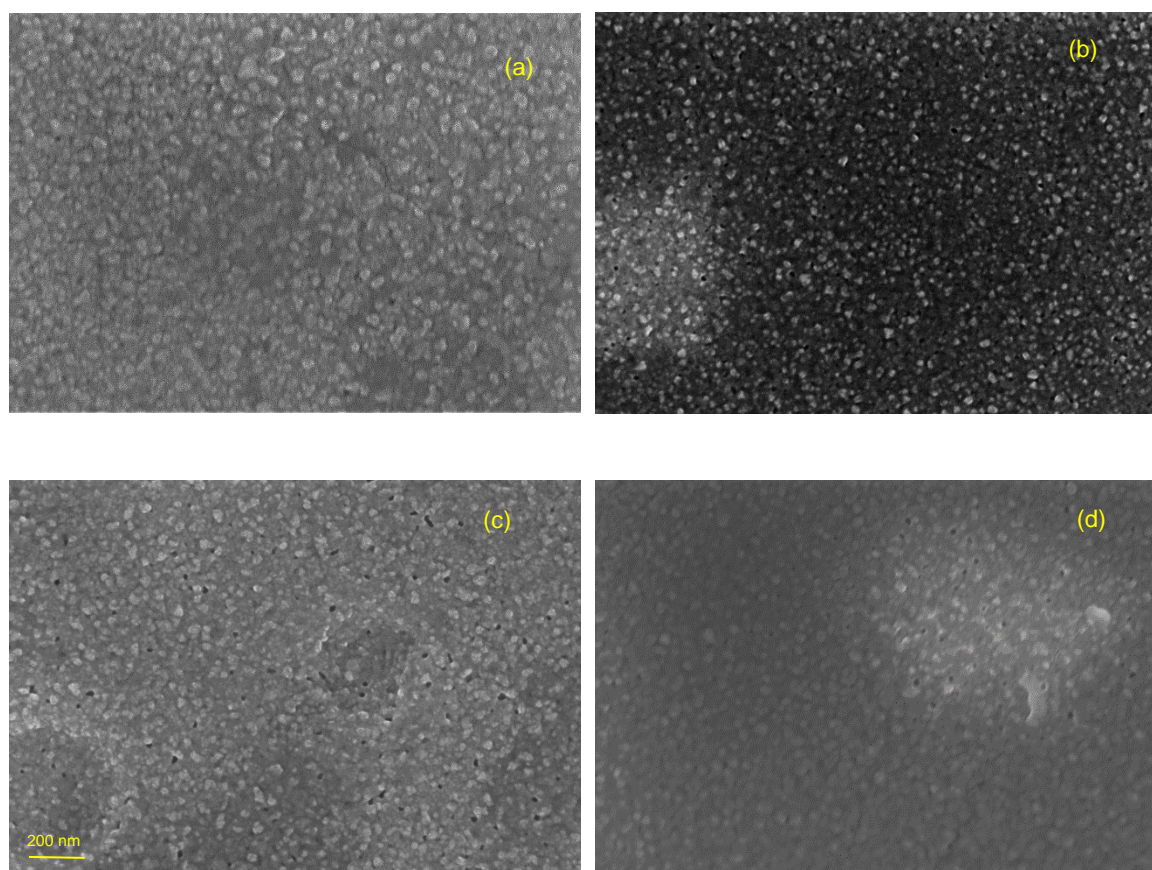


Figure 4 SEM images 150KX: a) EG; 150 – 350 – 750°C; b) EG; 350 – 750°C; c) EG – 2% Nb; 150 – 350 – 750°C; d) EG – 2% Nb; 350 – 750°C.

Finally, the Electric Field induced Polarization measurements (P vs E hysteresis loops) were obtained for all the fabricated devices. In Table 1 is reported the ratio between Delta remnant Polarization (ΔP_r) and Delta coercive field (ΔE_c) calculated according to the eq. 2:

$$\frac{\Delta P_r}{\Delta E_c} = \frac{P_r^+ - P_r^-}{E_c^+ - E_c^-} \quad \text{eq(2)}$$

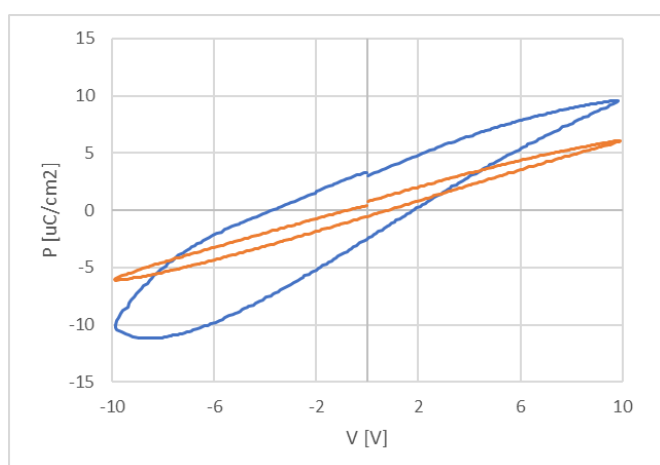


Figure 5. Comparison of PV loops of EG; 350 – 750°C (orange line) and EG – 2% Nb; 350 – 750°C (blue line).

No main differences have been obtained for the thin films characterized by the same material and different thermal treatment especially in the case of undoped material. Figure 5 reports the comparison of the PE loops of two devices with different material (doped vs undoped) and the same thermal treatment i.e. without the 1st hot plate. As clearly visible from the Figure 5, the doped material result in a large area of the loop which indicates that the volume of the ferroelectric domains that are switched by the external field is greater when the niobium is present. This fact is in line with the literature since the donor doping as in this case, increases the domains wall mobility (Akkopru-Akgun et al, 2019).x

4. Conclusions

In conclusion, sol gel thin films made of Barium Zirconate Titanate -Barium Calcium Titanate with 2% niobium doping were fabricated by repeated green chemical solution deposition routes. Moreover, we checked the possibility to simplify the process by removing the drying step. Characterizations indicated that morphology and electrical characterization of thin films are quite independent of the thermal treatment. While the effect of niobium doping improved the ferroelectric properties.

References

- Akkopru-Akgun B., Zhu W., Randall C.A., Lanagan M. T., Trolrier-McKinstry S., 2019, Polarity dependent DC resistance degradation and electrical breakdown in Nb doped PZT films *APL Materials*, 7, 120901-9, 2019.
- Aprea P., Liguori B., Caputo D., Casuscilli V., Cimmino A., di Matteo A., Salzillo G., 2017, Green Chemical Routes for the Synthesis of Lead-Free Ferroelectric Material $0.5\text{Ba}(\text{Zr}_{0.2}\text{Ti}_{0.8})\text{O}_3-0.5(\text{Ba}_{0.7}\text{Ca}_{0.3})\text{TiO}_3$, *Advanced Science Letters*, 23, 6015-6019.
- Barbato, P. S., Casuscilli, V., Aprea, P., Scaldaferrri, R., Caputo, D. 2021, a. Optimization of the production process of BZT–BCT sol–gel thin films obtained from a highly stable and green precursor solution. *Materials and Manufacturing Processes*, 36(14), 1642-1649.
- Barbato, P. S., Casuscilli, V., Aprea, P., Scaldaferrri, R., Pedaci, I., Caputo, D., 2021 b). Green Production of Lead-free BZT-BCT Thin Films for Applications in MEMS Devices. *Chemical Engineering Transactions*, 84, 97-102.
- Casuscilli V., Barbato P.S., Scaldaferrri R., Aprea P., Caputo D., 2023, Green, Homogeneous Solution for BZT-BCT Thin Film Deposition. *Lecture Notes in Electrical Engineering*, 918 LNEE, pp. 221–226.
- Hu P., 2018, Study on high precision mems inertial sensor with increased detection capacitance driven by electromagnetism, *Chemical Engineering Transactions*, 66, 1273-1278.
- Kang G., Yao K., Wang J., 2012 $(1-x)\text{Ba}(\text{Zr}_{0.2}\text{Ti}_{0.8})\text{O}_3-0.5(\text{Ba}_{0.7}\text{Ca}_{0.3})\text{TiO}_3$ ferroelectric thin films prepared from chemical solutions *Journal of American Ceramic Society*, 95, 986-991.B.
- Rödel J, Webber KG, Dittmer R, Jo W, Kimura M, Damjanovic D., 2015, Transferring lead-free piezoelectric ceramics into application. *Journal of European Ceramic Society*;35(6),1659–81.
- Shen Y., Liu Y., 2018, Properties of piezoelectric ceramics nanofilm from sol-gel process, *Chemical Engineering Transactions*, 66, 61-66.
- Trolrier-Mckinstry S., Muralt P., 2004, Thin Film Piezoelectrics for MEMS, *Journal of Electroceramics*, 12, 7-17.
- Wang Z., Zhaoc K., Guoa X., Wei Suna, Jianga H., Hana X., Taob X., Chengd Z., Zhaoef H., Kimurae H., Yuang G., Yinh J., Lihuh Z., 2013, Crystallization, phase evolution and f olution and ferroelectric pr oelectric properties of sol-gel- ties of sol-gel synthesized $\text{Ba}(\text{Ti}_{0.8}\text{Zr}_{0.2})\text{O}_3-x(\text{Ba}_{0.7}\text{Ca}_{0.3})\text{TiO}_3$ thin films *Journal of Materials Chemistry C*, 1, 522-530.
- Zhang C, Liu Q.B., Huand X. Q. Effect of sintering Temperature on Microstructure and electrical properties of (Mn, Nb)-Doped BZT-BCT Ceramics. *Adv. Mater. Res.* 820(2013), pp 59-62.